VERSITA

OPTO-ELECTRONICS REVIEW **14**(4), 269–273

DOI: 10.2478/s11772-006-0035-8

Design and simulation of single-electrode liquid crystal phased arrays

B. BELLINI*[1], M.A. GEDAY[1], N. BENNIS[1], A. SPADŁO[1], X. QUINTANA[1], J.M. OTÓN[1], and R. DĄBROWSKI[2]

[1]Dpto. Tecnología Fotónica, ETSI Telecomunicación, Universidad Politécnica de Madrid, Ciudad Universitaria s/n, E-28040 Madrid, Spain

[2]Institute of Chemistry, Military University of Technology, 2 Kaliskiego Str., 00-908 Warsaw, Poland

Liquid crystal (LC) phased arrays and gratings have been employed in optical switching and routing [1]. These diffractive optic elements are of great interest because they can be scaled up to a large number of elements and their optical properties can be electrically addressed with a low driving voltage. LC phase gratings have been achieved either by periodic addressing of pixels or by using periodically-modified structures. The latter approach leads to less reconfigurable devices but the addressing is simpler.

In this paper we focus on optical phased arrays where the phase is varied either continuously or discretely and where the periodicity is induced by electrode configuration. We first describe a possible structure based on a conductive silicon wafer. We argue that this structure can induce either continuously or discretely varying arrays while applying single voltage to the array. In the second part we simulate the behaviour of such arrays. We base the simulation on a LC synthesized at the Military University of Technology, this high-birefringence nematic LC shows in a 4-μm thick cell a linear phase shift range of more than 360° between 1.2 V and 1.8 V. We calculate the distribution of the LC molecule director and assess the performance of the array with respect to the applied voltage. Finally, the relevance of such technology for switchable phased arrays is discussed.

Keywords: liquid crystals, phased arrays, silicon.

1. Introduction

An optical phased array is an active diffractive optical element. It divides the wavefront of an incident beam in sub-beams (the pixels of the array) and changes their phase (and possibly amplitude and polarization). The pixels being of small dimensions, each sub-beam is diffracted. After the diffractive optical element, the interference pattern yields the output beam. The interference pattern depends on the phase shift at each pixel, therefore the shape and direction of the output beam can be dynamically addressed by addressing the light phase shift distribution at each pixel.

Various applications of optical phased arrays have been foreseen, interconnects, wavefront correcting, beam forming, and holography. Usually, all the pixels are independently addressed in order to get the highest degree of freedom in the diffractive properties, as in liquid crystal on silicon (LCoS, Ref. 2) technology. In a typical LCoS process, a pixel interconnect level, usually made up of aluminium lines, is placed on top of silicon. The whole is used as one of the cell substrates. LCoS phased arrays [3], microdisplays [4] have been demonstrated, design and fabrication issues have been discussed, e.g., in Refs. 5 and 6. The major issues are the ones of pixilated gratings, i.e., mainly pixel size, filling factor, and pixel complexity. However, for simple switchable or little tuneable phased arrays, a single electrode may be employed. In this sense, various technologies have been proposed, double perpendicular rubbing [7], corrugation of the alignment layer [8], and polymer-doped LC [9]. A common trait of these technologies is that there is no definition of individual pixels.

In this paper, we propose to form that kind of single electrode LC phased array on a silicon wafer. As an optical material, silicon exhibits interesting characteristics, it is transparent for wavelengths larger than 1.1 μm, has a refractive index of 3.45 at 1.5 μm, can be n- or p-doped, its native oxide is a good optical material of refractive index 1.45 at 1.5 μm. That is the reason why various waveguides and integrated optic devices have been fabricated in silicon on insulator (SOI) or silica on silicon [11]. Silicon is also expected to play the role of a photonic platform [12], integrating light waveguides, micromachined features and flip-chipped devices with silicon electronics.

In this paper, we will first give an insight of a possible design of a LC-on-silicon single electrode phased array. The director distribution in the LC layer will be simulated considering the case of a high-birefringence nematic liquid crystal and furthermore the characteristics of the diffraction pattern will be assessed.

*e-mail: bob.bellini@gmail.com

2. LC on silicon phased array

2.1. Model

A phosphorous-doped silicon wafer is used as a single electrode substrate where resistive regions can be locally defined either by ionic implantation or by oxidation. This property allows us to modify the electrostatic potential at the top of the substrate according to the importance of electrical isolation from the conductive wafer. Local change of the substrate electrical conductivity has also been reported on GaAs by electron-beam activation [13] or Si-ion implantation in non-intentionally-doped GaAs [14]. However, to our knowledge, ion-implantation for patterning a LC cell electrode, whose resistivity can be adjusted, has not been used on silicon substrate, yet. In addition, the proposed device on silicon is designed to be single electrode with a rear contact.

The geometry of a binary grating cell based on such a concept is shown in Fig. 1. When no voltage is applied, the LC is uniformly oriented and all the light is in the 0^{th} diffraction order (to the contrary of geometrically-textured arrays or multidomain alignment). When applying a voltage, the electric field drops over the neutral zone and is therefore periodically modified at the surface of the silicon substrate, inducing a periodical distribution of the molecular director. The diffraction efficiency in the 1^{st} order is maximum for a π-phase shift contrast.

In order to estimate the thickness of the isolated silicon, we consider a simple 1D dielectric model of the cell. If the voltage V_0 is applied to the conductive wafer, the voltage at the interface isolated silicon/LC is

$$V_1 = V_0 \frac{\frac{\varepsilon_1}{\varepsilon_2} d_2}{d_1 + \frac{\varepsilon_1}{\varepsilon_2} d_2}, \qquad (1)$$

where ε_1 is the dielectric constant of silicon, ε_2 is the average dielectric constant of the NLC, d_1 and d_2 are defined in Fig. 3.

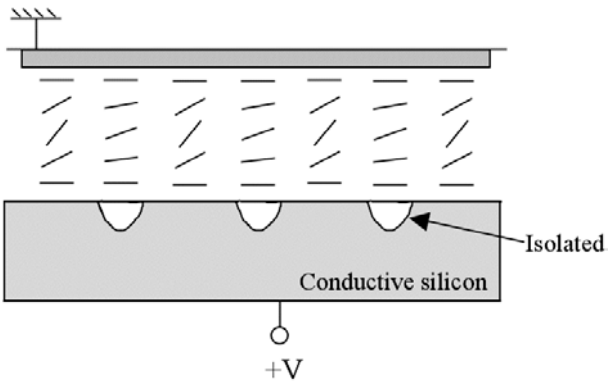

Fig. 1. Geometry of a cell on conductive silicon.

2.2. A required high-birefringence NLC

We consider the nematic liquid crystal (NLC) called 1660, synthesized at the Military University of Technology, which has the following characteristics, birefringence Δn = 0.38 at λ_0 = 0.633 m, k_{33}/k_{11} = 2.11, $\varepsilon_\perp$ = 5.1, and $\varepsilon_{||}$ = 9.4.

4-μm-thick cells have been fabricated, employing Nylon6 as alignment layer for homogeneous orientation. The phase shift in such cells (Fig. 2) has been measured at the wavelength λ_0 = 0.633 μm, using a Mach-Zehnder interferometer; the maximum phase shift is 4.2π rad. In the quasi-linear part, i.e., between the two operating points 1.2 V and 1.8 V applied voltage, the phase shift is more than 2π.

In a LC on Si cell, two configurations can be expected:

- transmission mode – for near infrared light we can choose a couple of applied voltages (after a graph such as the one of Fig. 2, but measured at the corresponding near infrared wavelength) for which a π-phase shift contrast can be achieved,
- reflection mode – it is suitable for visible light, where silicon is not transparent. The phase shift across the cell should be π/2.

In the following, reflection mode at λ_0 = 0.633 μm is used. From Fig. 2, V_0 = 1.57 V and V_1 = 1.33 V give a π-phase shift contrast, and the previous formula gives d_1 = 1.2 μm. In reflection, we need half the phase shift contrast,

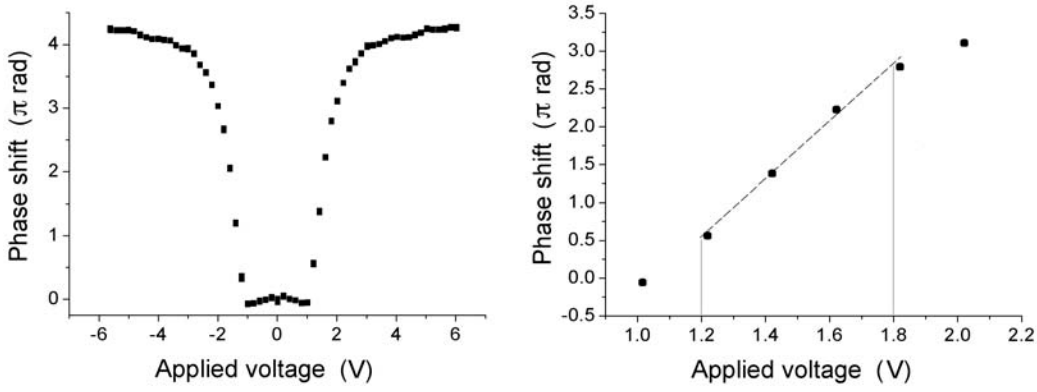

Fig. 2. Phase shift vs. applied voltage of a high-birefrigence LC. The cell is 4-μm thick. Left-hand side: full phase shift; right-hand side: zoom on the linear part.

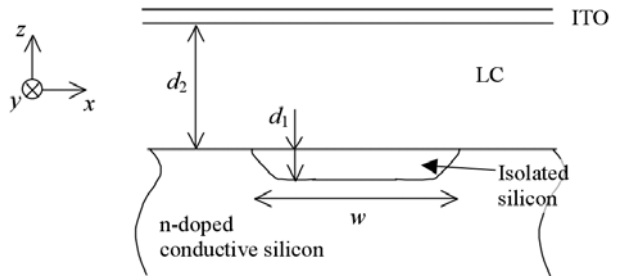

Fig. 3. Schematic of the cell.

which allows us to keep the same d_1 dividing the cell thickness roughly by 2. The value of d_1 is small enough to be achieved by ionic implantation. In the phase shift calculation we have also neglected the fringe effect, thus assuming that pixel dimensions are large compared to cell thickness.

Although this calculation is somewhat rough, it gives the order of magnitude of the insulation thickness and predicts that a large phase shift can be obtained between isolated and conductive regions by using a high-birefringence NLC.

2.3. Simulation of the phase shift at the output of the cell

The design and analysis of a LC phased array have been reported in many papers; for instance [15] presents a study of a pixelated blazed grating. The diffraction effect of the pixel patterning and calculation in a reflective cell have been also modelled [16].

We first want to validate the simulation on a uniform cell and retrieve the graph of Fig. 2. Afterwards we simulate the phased array.

The director distribution is simulated by means of LC3D software, from Kent University. The rubbing direction is assumed to be along *y*-axis and the tilt angle to be 2°. The software calculates the molecular director distribution, from which the refractive index distribution can be derived.

For a plane wave travelling in a medium, the phase shift can be calculated as

$$\delta\varphi = \frac{2\pi}{\lambda_0}\int n(z)dz, \qquad (2)$$

for a propagation along *z*-axis, *n* being the refractive index distribution (in this case, it only depends on *z*).

Applying this formula to the case of a single pad electrode, with incident light polarized along *y*-axis, gives the results shown in Fig. 4. The simulation does not perfectly fit the experiment, due to some non accurate (elastic constants) or undetermined (surface anchoring) LC parameters. In particular, the phase shift is steeper in the experiment, therefore the simulated device will need higher applied voltages.

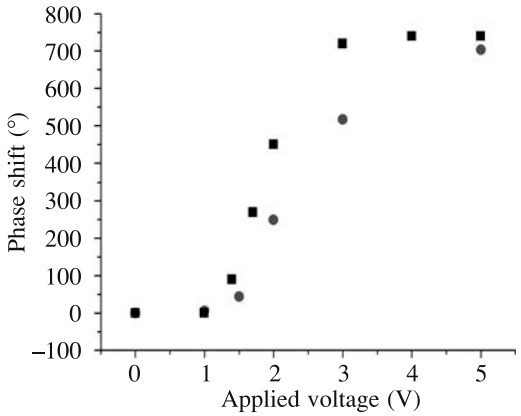

Fig. 4. Phase shift after the 1660 NLC cell: measured (squares) and simulated (disks).

We now simulate one grating period. Due to the fringe effects light propagating in the cell is not *a priori* a plane wave anymore. Then, we simulate the propagation by a two-dimensional beam propagation method (2D BPM) whose algorithm is based on finite differences. As the cell is not too thick, the paraxial approximation is still valid. Figure 5 shows the light phase at the output of the cell, as calculated by the previous formula and as calculated after BPM simulation. To get a π-phase shift (after return pass) we had to assume a 1.95 V applied voltage in the neutral zone, and 1.5 V in the rest.

A binary grating was built, with a period of 20 μm and 10 μm-wide insulation zones. An incident plane wave thus comes out of the grating with a modulated phase as represented in Fig. 6, which can be compared to the ideally-squarred case where there is no fringe effect.

2.4. Diffraction pattern

The diffraction patterns correspond to a 20-period grating (400 μm wide) and are calculated in Fraunhoffer approximation (far field), considering the difference of amplitude

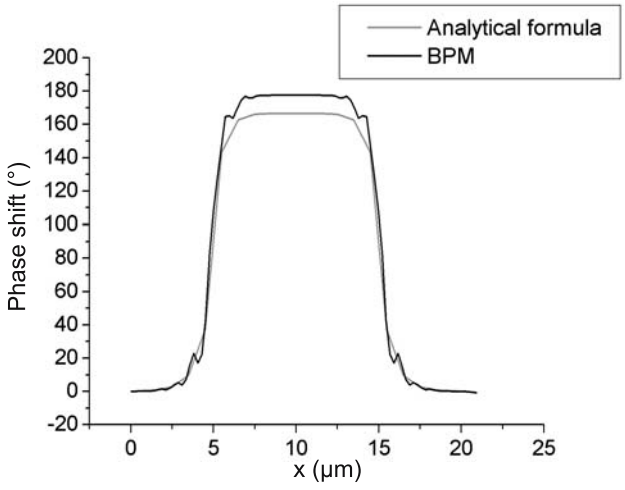

Fig. 5. Phase shift after a 4-μm-thick, single pad cell, calculated by 2D BPM.

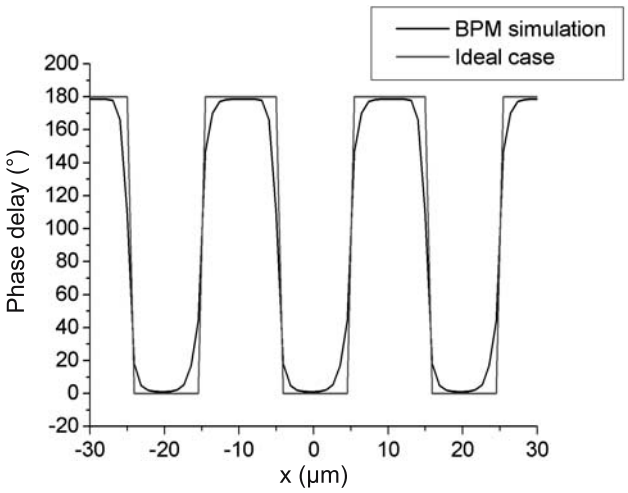

Fig. 6. Binary phase grating: after direction simulation and BPM phase calculus, and ideal case.

reflection coefficient between conductive and isolated silicon (for optical properties of silicon, see for example Ref. 17 and papers by the same author).

When no voltage is applied, only the 0th diffraction order is present. The diffraction pattern appears when applying a voltage on the silicon wafer. Figure 7 shows the patterns for a π-phase shift modulation, in the ideal and practical cases. Both have symmetric patterns.

In the ideal case, only odd diffraction orders are present. The main consequence of considering the fringe effect is the appearance of the 0th and even diffraction order. In the 1st order though, the power is only decreased by 0.1 dB, with respect to the ideal case. Furthermore, considering fringe effect, the crosstalk (ratio between the intensities in the 0th and 1st order mode) is 9.7 dB.

By varying the applied voltage, intermediate cases can be reached, for instance a multi-cast phased array, i.e., an array dividing the power equally between different orders (0 and +/–1). Such a phased array may then be suitable in cases of routing and casting where the crosstalk is not a crucial specification. It can also be noted that the diffraction pattern can be made highly asymmetric (more intensity in order 1 than in order –1) just by modifying the alignment layer, namely rubbing direction and tilt angle [18].

3. Conclusions

We have presented a novel design of liquid crystal phased array. The objective is to control the array by a single electrode, in this case a conductive silicon wafer, by introducing isolated zones by ionic implantation. The design is simple and the technology reduced, in order to achieve low-cost power dividers. Furthermore, the use of silicon permits to integrate the array with electronic or integrated optic on silicon circuits.

Such phased arrays can operate in transmission or reflection. The use of high-birefringence nematic liquid crystals permits to have thickness of insulated zones of the order of the micron, and to reduce the cell thickness. After liquid crystal orientation and light propagation simulations, the diffraction patterns have been computed, they show that limited fringe effect and moderate crosstalk can be achieved.

Acknowledgments

Part of the study has been done under the SAMPA project (European Training and Mobility Research network). Financial support of Spanish Ministerio de Educación y Ciencia (project TEC2005-08218-C02-01) is acknowledged.

References

1. J.L. De Bougrenet De La Tocnaye, "Engineering liquid crystals for optimal uses in optical communication systems", *Liq. Cryst.* **31**, 241–269 (2004).
2. K.M. Johnson, D.J. McKnight, and I. Underwood, "Smart spatial light modulators using liquid crystals on silicon", *IEEE J. Quant. Electron.* **29**, 699–714 (1993).
3. S. Serati and J. Stockley, "Advanced liquid crystal on silicon optical phased arrays", *IEEE Aerospace Conf. Proc.* **3**, 1395–1402 (2002).
4. H.S. Kwok and H.C. Huang, "Liquid crystal on silicon microdisplays", *Proc. 7th Int. Conf. on Solid-State and Integrated Circuit Technology* **3**, 1987–1990 (2004).

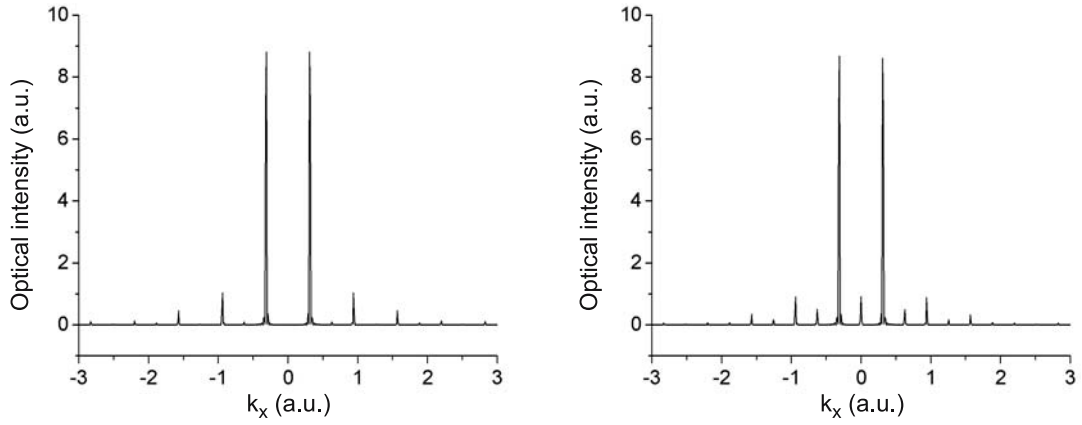

Fig. 7. Calculated diffraction patterns of the binary phase grating, without (left-hand side) and with (right-hand side) fringe effect.

5. D.J. McKnight, K.M. Johnson, and R.A. Serati, "256×256 liquid-crystal-on-silicon spatial light modulator", *Appl. Opt.* **33**, 2775–2784 (1994).
6. H. De Smet, D. Cuypers, A. Van Calster, J. Van den Steen, and G. Van Doorselaer, "Design, fabrication and evaluation of a high-performance XGA VAN-LCOS microdisplay", *Displays* **23**, 89–98 (2002).
7. J. Chen, P.J. Bos, H. Vithana, and D.L. Johnson, "An electro-optically controlled liquid crystal diffraction grating", *Appl. Phys. Lett.* **67**, 2588–2590 (1995).
8. M. Honma and T. Nose, "Polarization-independent liquid crystal grating fabricated by microrubbing process", *Jap. J. Appl. Phys.* **42**, 6992–6997 (2003).
9. R. Caputo, L. De Sio, A.V. Sukhov, N.V. Tabirian, A. Veltri, and C. Umeton, "Realization of a new kind of switchable holographic grating made of liquid crystal films separated by slices of polymeric material (POLICRYPS)", *Opt. Lett.* **29**, 1261–1263 (2004).
10. D.X. Xu, P. Cheben, B. Lamontagne, S. Janz, and W.N. Ye, "Silicon-on-insulator (SOI) as a photonic platform", *207th ECS Meeting*, 554 (2005).
11. L. Wosinski, "Silica-on-silicon technology for photonic integrated devices", *Proc. 6th Int. Conf. on Transparent Optical Networks* **2**, 274–279 (2004).
12. B. Bellini, J.F. Larchanché, J.P. Vilcot, D. Decoster, R. Beccherelli, and A. d'Alessandro, "Photonic devices based on preferential etching", *Appl. Optics* **44**, 7181–7186 (2005).
13. L. Kurowski, D. Bernard, E. Constant, and D. Decoster, "Electron-beam-induced reactivation of Si dopants in hydrogenated two-dimensional AlGaAs heterostructures: a possible new route for III-V nanostructure fabrication", *J. Phys. Cond. Mat.* **16**, S127–S132 (2004).
14. D.P. Resler, D.S. Hobbs, R.C. Sharp, L.J. Friedman, and T.A. Dorschner, "High-efficiency liquid crystal optical phased-array beam steering", *Opt. Lett.* **21**, 689–691 (1996).
15. G.F. Barrick, P.J. Bos, C.E. Titus, and B.K. Winker, "Computing the liquid crystal director field in optical phased arrays", *Opt. Eng.* **43**, 924–932 (2004).
16. K.H. Fan Chiang, S.H. Chen, and S.T. Wu, "Diffraction effect on high-resolution liquid-crystal-on-silicon devices", *Jap. J. Appl. Phys.* **44**, 3068–3072 (2005).
17. R.A. Soref and J.P. Lorenzo, "All-silicon active and passive guided-wave components for λ = 1.3 and 1.6 μm", *IEEE J. Quant. Electron.* **22**, 873–879 (1986).
18. C.V. Brown, E.E. Kriezis, and S.J. Elston, "Optical diffraction from a liquid crystal phase grating", *J. Appl. Phys.* **91**, 3495–3500 (2002).